Silencing of SIVA-1 promotes cisplatin resistance in gastric cancer via the Bcl-2/BAX-mediated mitochondria-dependent apoptosis pathway

ZHENG-YI SHI[1,2*], ZHENG-RONG DING[3*], YU-LIANG HUANG[1], YUAN-RUI LEI[2,4], HAI-BIN HUANG[1,2], YAN QING[1], MIAO-REN DENG[1,2], XU-MAN LU[4], XU-DONG DONG[1], LONG-JIE XIA[5], SHENG XU[4], XIAO-GANG ZHONG[4], LEI LI[4], FAN-BIAO KONG[1] and XIAO-TONG WANG[4]

[1]Department of Colorectal and Anal Surgery, People's Hospital of Guangxi Zhuang Autonomous Region and Institute of Minimally Invasive Technology and Applications, Guangxi Academy of Medical Sciences, Nanning, Guangxi Zhuang Autonomous Region 530021, P.R. China; [2]Graduate School, Guangxi Medical University, Nanning, People's Republic of China, Guangxi Zhuang Autonomous Region 530021, P.R. China; [3]The Tenth Clinical Medical College of Guangzhou University of Traditional Chinese Medicine, Zhongshan Hospital of Traditional Chinese Medicine, Zhongshan, Guangdong 528400, P.R. China; [4]Departments of Gastrointestinal, Hernia and Enterofistula Surgery, People's Hospital of Guangxi Zhuang Autonomous Region and Institute of Minimally Invasive Technology and Applications, Guangxi Academy of Medical Sciences, Nanning, Guangxi Zhuang Autonomous Region 530021, P.R. China; [5]Department of Cosmetic Plastic Surgery, People's Hospital of Guangxi Zhuang Autonomous Region, Guangxi Academy of Medical Sciences, Nanning, Guangxi Zhuang Autonomous Region 530021, P.R. China

Received June 13, 2025; Accepted January 7, 2026

DOI: 10.3892/or.2026.9100

Abstract. The aim of the present study was to investigate the effects of SIVA-1 silencing on the drug resistance and biological functions of cisplatin (DDP)-resistant human gastric cancer cells (AGS/DDP), and to explore the mechanism underlying its occurrence. AGS/DDP cells with stable silencing of SIVA-1 were established by molecular biology techniques. The Cell Counting Kit-8 assay was used to investigate the effect of SIVA-1 silencing on drug sensitivity in AGS/DDP cells by measuring the IC_{50} of Adriamycin, DDP and vincristine. The findings demonstrated that the suppression of SIVA-1 in AGS/DDP cells markedly augmented the resistance to DDP. In addition, cell proliferation, cell migration, cell invasion and cell apoptosis were assessed using colony formation, cell scratch, Transwell and cell apoptosis assays, respectively. The results of these assays demonstrated that silencing SIVA-1 notably increased the proliferation, migration and invasion of AGS/DDP cells, while concurrently inhibiting their apoptosis. Furthermore, the effects of SIVA-1 silencing on drug-resistant gastric cancer cells *in vivo* were confirmed using a subcutaneous xenograft model in nude mice. The results demonstrated that silencing SIVA-1 led to a notable increase in tumor volume, growth rate and weight. The bioinformatics analyses results indicated that SIVA-1 may have an interactive relationship with Bcl-2, BAX, X-linked inhibitor of apoptosis protein (XIAP), MAPK8 and baculoviral inhibitor of apoptosis repeat-containing 5 (BIRC5), and could participate in the mitochondria-dependent apoptosis pathway. The results of reverse transcription-quantitative PCR and western blotting indicated that silencing SIVA-1 in AGS/DDP cells promoted the expression levels of Bcl-2, XIAP, MAPK8 and BIRC5, and inhibited the expression levels of BAX. In conclusion, silencing SIVA-1 has been shown to modify sensitivity to DDP and biological function in drug-resistant gastric cancer cells, either directly or indirectly. This phenomenon may be associated with the Bcl-2/BAX-mediated, mitochondria-dependent apoptosis pathway.

Correspondence to: Dr Xiao-Tong Wang, Departments of Gastrointestinal, Hernia and Enterofistula Surgery, People's Hospital of Guangxi Zhuang Autonomous Region and Institute of Minimally Invasive Technology and Applications, Guangxi Academy of Medical Sciences, 6 Taoyuan Road, Nanning, Guangxi Zhuang Autonomous Region 530021, P.R. China
E-mail: 008.wxt@163.com

Dr Fan-Biao Kong, Department of Colorectal and Anal Surgery, People's Hospital of Guangxi Zhuang Autonomous Region and Institute of Minimally Invasive Technology and Applications, Guangxi Academy of Medical Sciences, 6 Taoyuan Road, Nanning, Guangxi Zhuang Autonomous Region 530021, P.R. China
E-mail: kfb.32@163.com

*Contributed equally

Key words: drug resistance, gastric cancer, SIVA-1, Bcl-2, bioinformatics analysis

Introduction

Gastric cancer is a prevalent malignancy within the digestive system. According to data from a global burden of disease

study (1), compared with in 1990, there were an estimated 1.23 million new cases of gastric cancer and 954,000 gastric cancer-related deaths worldwide in 2021. According to data from the American Cancer Society (2), there were an estimated 1.23 million new gastric cancer cases and 954,000 gastric cancer-related deaths in the United States in 2024. This demonstrates that gastric cancer remains a notable global health concern.

One of the major challenges in the treatment of gastric cancer is cisplatin resistance (3). The mechanisms that lead to drug resistance are complex and diverse, involving multiple aspects, such as increased drug efflux and the upregulation of DNA damage repair capabilities. Enhanced drug efflux is mainly mediated by upregulation or increased activity of ABC transporters, leading to a decrease in intracellular drug concentration (4,5). Notably, experimental findings by Chen *et al* (6) demonstrated that the upregulation of NBS1 can increase the DNA damage repair capacity, consequently enhancing chemotherapy resistance (6). Moreover, the targeting and downregulation of checkpoint kinase 1 has been demonstrated to be an efficacious method of reversing drug resistance in gastric cancer cells (7). SIVA-1, a pro-apoptotic protein that can be activated by the P53 tumor suppressor protein (8), has been demonstrated to be associated with the induction of apoptosis in a variety of tumor cells, such as breast cancer (9), ovarian cancer (10) and glioblastoma (11). Previous experimental results have demonstrated that SIVA-1 serves an important role in reversing the sensitivity of gastric cancer-resistant cells to vincristine (VCR) (12,13). However, the effects of SIVA-1 silencing on the drug sensitivity and biological function of cisplatin (DDP)-resistant human gastric cancer cells (AGS/DDP) remain to be elucidated, and the mechanisms underlying altered drug sensitivity must be explored. In the present study, AGS/DDP cells, in which SIVA-1 was silenced, were constructed, and the changes in the sensitivity of the cells to drugs, and alterations in their proliferation, migration and invasion were observed, to assess the role of SIVA-1 in gastric cancer chemoresistance.

Materials and methods

Bioinformatics analysis. The stomach adenocarcinoma (STAD) transcriptome dataset in The Cancer Genome Atlas (TCGA; https://portal.gdc.cancer.gov/) was acquired, which contains data from 379 gastric cancer tissue and 34 normal gastric tissue. The GSE186205 (14) dataset was acquired from the Gene Expression Omnibus (https://www.ncbi.nlm.nih.gov/geo). The GSE186205 dataset contains one immortalized gastric cancer cell line (KATOIII) and one immortalized cisplatin-resistant gastric cancer cell line (KATO/DDP), with the experiment repeated three times. The R 4.2.3 software (https://cran.r-project.org/bin/windows/base/old/4.2.3/) was used for analysis. The 'DESeq2' package (version 1.40.2) (15) was used to analyze the differential genes between the tumor group and the drug-resistant group in the GSE186205 dataset. $P<0.05$ and absolute log2(FoldChange)>2 were considered to indicate differentially expressed genes. The inter-group risk scoring of the SIVA-1 gene in TCGA-STAD was performed using the 'survival' package (https://github.com/therneau/survival), and the impact of SIVA-1 expression levels on overall patient survival was assessed using a Cox proportional hazards regression model. Data visualization was performed using the 'ggrisk' package (https://github.com/yikeshu0611/ggrisk). The gene-drug correlation of SIVA-1 in the GSE186205 dataset was analyzed using the oncoPredict package (16) and a scatter plot of the results of the Pearson correlation analysis was generated. A comprehensive search was conducted in the STRING 12.0 database (https://cn.string-db.org/) for SIVA-1, Bcl-2, BAX, X-linked inhibitor of apoptosis protein (XIAP), MAPK8 and baculoviral inhibitor of apoptosis repeat-containing 5 (BIRC5), with a minimum required interaction score of 0.40. The output of this analysis showed the six protein interactions using Cytoscape 3.10.3 (https://cytoscape.org/), and protein-protein interaction (PPI) networks were plotted. The MSigDB database (http://www.gsea-msigdb.org/gsea/msigdb/index.jsp) was used for Gene Set Enrichment Analysis (GSEA). Gene Ontology (GO) and Kyoto Encyclopedia of Genes and Genomes (KEGG) enrichment analyses were performed using the 'clusterProfiler' package (17), with GO enrichment analysis including biological process (BP), cellular component (CC) and molecular function (MF) terms. The GSEA, and KEGG and GO enrichment analyses were used to analyze the GSE186205 dataset. Functional pathways with filter-corrected $P<0.05$ and $q<0.05$ were considered to be differential. Subsequently, the GO enrichment data were visualized using the 'ggSankey' package (https://github.com/davidsjoberg/ggsankey).

Reagents. DDP (cat. no. H20073653) and Adriamycin (ADM) were procured from Qilu Pharmaceutical Co., Ltd. Trypsin, streptomycin, penicillin and VCR were procured from Sigma-Aldrich; Merck KGaA. The following antibodies were procured from Cell Signaling Technology, Inc.: SIVA-1 (cat. no. 12532S), Bcl-2 (cat. no. 4223S), BAX (cat. no. 2772S), MAPK8 (cat. no. 3708S), BIRC5 (cat. no. 8756S), XIAP (cat. no. 2042S) and GAPDH (cat. no. 5174). The SIVA-1 RNA interference (RNAi) recombinant lentiviral vector [pGV358-GFP-SIVA-1-short hairpin RNA (shRNA)] and the null vector [pGV358-GFP-negative control (NC)] were obtained from Shanghai Jikai Gene Medical Technology Co., Ltd.

Cell culture. AGS/DDP cells (cat. no. KGG3506-1) were procured from Nanjing KeyGen Biotech Co., Ltd., and cultured in RPMI 1640 medium (Thermo Fisher Scientific, Inc.), which was supplemented with 10% FBS (Thermo Fisher Scientific, Inc.) and antibiotics (100 U/ml penicillin + 100 mg/ml streptomycin). The cells were cultured at 37˚C under 5% CO_2 gas conditions. To maintain the drug-resistant phenotype, AGS/DDP cells were cultivated in medium augmented with 0.6 μg/ml DDP. The 293T cells were obtained from the Xiangya Center Laboratory at Central South University (Changsha, China).

Infection with the shRNA-SIVA-1 lentiviral vector and formation of stably silenced expression cell lines. The pGV358-GFP-SIVA-1-shRNA and pGV358-GFP-NC were separately co-transfected with pHelper 1.0 and pHelper2.0 into 293T cells using a second-generation lentiviral vector system. The total amount of lentiviral vector, and pHelper 1.0 and pHelper 2.0 plasmid DNA was 45 μg, with a mass

ratio of 2:1.5:1. The mixture (lentiviral vector, pHelper 1.0 and pHelper 2.0), Lipofectamine® 3000 Transfection Reagent (cat. no. L3000015; Invitrogen; Thermo Fisher Scientific, Inc.) and Opti-MEM™ medium (cat. no. 31985062; Gibco; Thermo Fisher Scientific, Inc.) were added to a 6-well plate containing 293T cells, and the plate were incubated at 37˚C in a 5% CO_2 incubator. A total of 6 h post-transfection, the medium was replaced with fresh DMEM (Hyclone™; Cytiva), and the cells were cultured for an additional 4 days before viral supernatant collection. Lentiviral particles were harvested by ultracentrifugation (53,780 x g, 2 h, 4˚C). The viral titer (Lv-SIVA-1-shRNA and Lv-NC) was measured by fluorescence microscopy (Keyence Corporation). The titer of the concentrated lentiviral particles (Lv-SIVA-1-shRNA and Lv-NC) was determined using a gradient dilution method and was calculated to be $2x10^9$ TU/ml. AGS/DDP cells were then transduced with Lv-SIVA-1-shRNA and Lv-NC recombinant lentiviruses particles at a multiplicity of infection of 30 for a period of 48 h at 37˚C. Stable cell line selection commenced 72 h after transduction of AGS/DDP cells with lentiviral particles. After being treated with 0.6 μg/ml DDP, the cell lines exhibiting stable silencing of SIVA-1 were then subjected to a 4-week screening process using 5 μg/ml puromycin for initial selection, followed by maintenance at a concentration of 3 μg/ml puromycin. Following the completion of this screening phase, the AGS/DDP cells were divided into the following three distinct groups based on the outcomes obtained: i) shRNA-SIVA-1 group; ii) shRNA-NC group; and iii) control group (uninfected).

Cell viability assay. Following cell recovery via thawing in a 37˚C water bath and centrifugation at 100 x g for 5 min, cell digestion was performed using 0.5% trypsin-EDTA (Thermo Fisher Scientific, Inc.) at 37˚C and was terminated with medium containing 10% FBS. The resulting cell pellets were then resuspended in RPMI 1640 medium and the cell concentration was adjusted to $1.5x10^4$ cells/ml. The cells in the shRNA-SIVA-1, shRNA-NC and control groups were inoculated in 96-well plates (~5,000 cells/well) and were placed in a cell culture incubator set to 37˚C with 5% CO_2. Following a 24-h incubation period, cell viability was assessed after treatment with DDP (0-500 μg/ml), ADM (0-1,000 μg/ml) and VCR (0-850 μg/ml) at 37˚C for 48 h. Briefly, 10 μl Cell Counting Kit-8 reagent (Dojindo Laboratories, Inc.) was added and the cells were incubated at 37˚C for 2 h. Subsequently, the IC_{50} of each group was analyzed and calculated at 450 nm using a microplate reader (PR 3100 TSC; Bio-Rad Laboratories, Inc.).

Colony formation assay. The colony formation assay is a reliable method for assessing the proliferative capacity of cells. Following the completion of cell recovery and cell digestion, cells from the shRNA-SIVA-1, shRNA-NC and control groups were inoculated in 6-well plates (~500 cells/well). The cells were cultured at 37˚C in the presence of DDP (0.6 μg/ml), under humidified 5% CO_2 gas conditions for 2 weeks, during which the complete medium was changed every 3 days. Subsequently, the cells were fixed with 500 μl 4% paraformaldehyde/well at 37˚C for 30 min, and stained with 500 μl 0.5% crystal violet staining solution/well at 37˚C for 5 min after washing twice with PBS. Colony formation was manually counted under an inverted optical microscope (CKX53; Olympus Corporation) at x40 magnification. Colonies were defined as clusters containing ≥50 cells. The colony formation rate (%) was calculated using the formula: (number of colonies formed/total number of cells inoculated) x100.

Cell apoptosis assays. To detect the effects of silencing SIVA-1 on the apoptosis of AGS/DDP cells, each group of cells was treated with 20 μg/ml DDP. To illustrate more clearly the changes in apoptosis caused by variations in cisplatin sensitivity among the groups, a concentration of 20 μg/ml (close to the IC_{50} concentration) was selected for this assay. The Annexin V-PE/7-AAD Apoptosis Kit (cat. no. AP-105; Hangzhou Lianke Biotechnology Co., Ltd.) was then utilized in accordance with the manufacturer's guidelines. The cells were incubated with 1X Binding Buffer containing Annexin V-PE and 7-AAD for 15 min at 25˚C in the dark. Subsequently, the stained cells were detected by flow cytometry using a FACScan instrument (Agilent Technologies, Inc.) and data analysis was performed using MultiCycle for Windows (version AV; Phoenix Flow Systems).

Cell scratch assay. The cell scratch assay is a well-established *in vitro* experiment that models the process of cell migration. Following completion of the cell recovery and cell digestion procedures, cell growth was observed continuously on a daily basis. The cells were seeded in 12-well plates until they reached 90-95% confluence, after which, a sterile pipette tip was used to create a linear wound in the center of the confluent cells, and the cells were rinsed twice with PBS to remove cell debris. Subsequently, the cells were cultured in serum-free medium. The healing process was observed under x40 magnification using an inverted optical microscope (CKX53; Olympus Corporation) at 0, 24 and 48 h, respectively. The area of the scratches was measured using the microscope companion software (Confluency Checker Software; version 1.2; Olympus Corporation). Wound healing (%) was calculated as follows: (0-h scratch area-48-h scratch area)/0-h scratch area x100.

Transwell assay. The capacity of cells to migrate or invade was evaluated by employing a 24-well Transwell system (8.0 μm pore polycarbonate membrane; cat. no. 3422; Corning Inc.), which served to replicate the physiological conditions under which cells traverse *in vivo* tissues. Initially, 500 μl complete medium containing 10% FBS was added to the lower chamber of a 24-well plate, and a Transwell chamber was placed above it. For the invasion assay, 100 μl diluted Matrigel was added and cured at 37˚C for 1 h to form a gel matrix. Following the completion of cell recovery and cell digestion, the cells in the shRNA-SIVA-1, shRNA-NC and control groups were inoculated in the upper chamber of the 24-well plate (~$5x10^4$ cells/well), and the plate was returned to the incubator to continue cultivation. After 24 h, the Transwell chamber was fixed in 400 μl 4% paraformaldehyde at room temperature for 10 min, washed once with PBS and stained with 400 μl crystal violet at room temperature for 5 min. Subsequently, the chambers were washed three times, both internally and externally, with PBS. The number of visible cells that had migrated/invaded the membrane was subsequently observed under an inverted optical microscope (CKX53; Olympus

Corporation) at x40 magnification. For the cell migration assay, the aforementioned protocol was repeated in the absence of Matrigel.

Reverse transcription-quantitative PCR. After completion of cell recovery and cell digestion, the cell concentration was adjusted to $1.5x10^4$ cells/ml. Total RNA was extracted from cells in all groups (shRNA-SIVA-1, shRNA-NC and control) using Triquick Reagent (cat. no. R1100; Beijing Solarbio Science & Technology Co., Ltd.) according to the manufacturer's instructions. Specifically, RNA Extraction Reagent (cat. no. P1011; Beijing Solarbio Science & Technology Co., Ltd.) was added during the phase separation step. The extracted RNA was then reverse transcribed into cDNA using the Reverse Transcription Kit (cat. no. MR05101M; Monad Biotech Co., Ltd.) according to the manufacturer's protocol. qPCR was performed using the 2X S6 Universal SYBR qPCR Mix [cat. no. Q204-01; XinBei Biotechnology (Suzhou) Co., Ltd.] on a Real-Time PCR System (MA-6000; Molarray Research, Inc.) under the following thermocycling conditions: Initial denaturation at 95˚C for 30 sec, followed by 40 cycles of denaturation at 95˚C for 3-10 sec and annealing/extension at 60˚C for 10-30 sec. The primers for PCR are shown in Table I. Relative gene expression levels were calculated using the $2^{-\Delta\Delta Cq}$ method (18) with GAPDH as the internal reference gene. The experiment was repeated three times, with the mean value taken as the final result.

Table I. Primer sequences used for reverse transcription-quantitative PCR.

Gene	Base sequence, 5'-3'
SIVA-1	F: GTCGTTCACCTGCCAGAGTC
	R: CCGTCTGGTCCAATCAGCAT
MAPK8	F: CTTGGCATGGGCTACAAGGA
	R: GGTGGGGACATAAGGTGGTG
Bcl-2	F: GTGTGTGGAGAGCGTCAACC
	R: ACAGTTCCACAAAGGCATCC CAG
BAX	F: AGTAACATGGAGCTGCAGAGGA TGA
	R: TGGAGACAGGGACATCAGTCG
XIAP	F: ATTTCCAGATTGGGGCTCGG
	R: CTTGTCCACCTTTTCGCGCC
BIRC5	F: CCACTGAGAACGA GCCAGACTT
	R: GTATTACAGGCGTAAGCCACCG
GAPDH	F: TGACGTGGACATCCGCAAAG
	R: CTGGAAGGTGGACAGCGAGG

BIRC5, baculoviral inhibitor of apoptosis repeat-containing 5; F, forward; R, reverse; XIAP, X-linked inhibitor of apoptosis protein.

Western blotting. After cell recovery and digestion, total proteins were extracted from whole cell lysates using RIPA Lysis and Extraction Buffer (cat. no. 89901; Thermo Fisher Scientific, Inc.). The concentration of the extracted proteins was measured using the BCA Protein Quantification Kit (Thermo Fisher Scientific, Inc.). The absorbance value of each sample was measured at 562 nm using a microplate reader and the concentration was calculated from the standard curve. Total proteins (20 μg) were collected for SDS-PAGE on 10% gels and were transferred onto a PVDF membrane, before being incubated with QuickBlock™ Blocking Buffer (cat. no. P0235; Beyotime Biotechnology) for 1 h at room temperature with agitation. The following primary antibodies were then added and incubated overnight at 4˚C with agitation: Anti-SIVA-1 (1:500), anti-Bcl-2 (1:500), anti-BAX (1:500), anti-MAPK8 (1:1,000), anti-BIRC5 (1:500), anti-XIAP (1:1,000) and anti-GAPDH (1:1,000). Subsequently, Goat Anti-Rabbit IgG H&L (HRP) (cat. no. ab6721; Abcam) was added and incubated for 1 h at room temperature in the dark, and washed three times with 0.1% TBS Tween-20 Buffer (cat. no. 28360; Thermo Fisher Scientific, Inc.). A gel imager (iBright CL750; Invitrogen; Thermo Fisher Scientific, Inc.) was used to scan the protein blotting membrane, and the gray scale values of the bands were analyzed and recorded using ImageJ software (bundled with 64-bit Java 8; National Institutes of Health). The relative expression levels of the target proteins were expressed as the ratio of the integrated optical densities of the target protein bands and the GAPDH bands.

Establishment of a subcutaneous tumor xenograft model in nude mice. Ethics approval for the animal experiments in the present study was obtained from The Medical Ethics Committee of People's Hospital of Guangxi Zhuang Autonomous Region (approval no. KY-GZR-2016-416; Nanning, China). A total of 30 5-week-old male BALB/c nude mice (weight, 16-18 g), were purchased from Beijing Vital River Laboratory Animal Technology Co., Ltd., and maintained at the Laboratory Animal Center of Guangxi Medical University (Nanning, China). The housing environment was maintained at a temperature of 22±2˚C and a relative humidity of 55±10%, with a 12-h light/dark cycle. Autoclaved standard rodent diet and sterile drinking water were provided *ad libitum*. The nude mice were subcutaneously inoculated with AGS/DDP cells ($2x10^6$ cells in 100 μl suspension/mouse) into the left anterior abdomen. The health status and behavior of the nude mice were monitored daily. According to the animal operational procedures established by the Animal Ethics Committee of the People's Hospital of Guangxi Zhuang Autonomous Region, a standardized management plan was put in place to deal with any in-fighting as followed: i) The immediate separation of involved animals and tiered intervention based on the severity of the wounds; ii) superficial wounds were treated with topical cleansing and antisepsis; iii) severe trauma cases were assessed by a veterinarian to determine the appropriateness of euthanasia; and iv) animals were humanely euthanized once they reached predefined humane endpoints (19-22). The presence of a tumor measuring ≥1.5 cm in any direction, accompanied by body weight loss of >20% of the initial weight, or 10% weight loss accompanied by severe clinical signs of distress (such as hypotrichosis, loss of appetite or reduced vitality), were considered humane endpoints. If mice reached these endpoints they were euthanized (23). When the resulting tumor diameter was measured to be 5 mm, the mice were randomly divided into the following three groups (n=10/group): i) shRNA-SIVA-1

group; ii) shRNA-NC group; and iii) control group. Nude mice in the shRNA-SIVA-1 group or the shRNA-NC group were injected intratumorally with 100 μl Lv-SIVA-1-shRNA or Lv-NC recombinant lentivirus particles every 2 days. Each injection consisted of 100 μl lentiviral suspension with a titer of $2x10^9$ TU/ml. When the subcutaneous xenografts were visible, the length and width of the tumor were measured every 2 days. Tumor volume was calculated using the following formula: Length x $width^2$ x0.5 cm^3. The relative tumor volume (RTV) was calculated on day 13 using the following formula: Tumor volume on day 13/tumor volume before administration. DDP was injected intraperitoneally at a dose of 3 mg/kg every 2 days. A total of 13 days after tumor injections, the mice were sacrificed by cervical dislocation. Death was confirmed by the absence of vital signs (respiratory arrest, loss of corneal reflex and no response to a toe pinch), the xenografts were dissected and harvested for further analysis. Only mice that survived until the end of the experiment were included in the tumor growth and parameter analysis.

Hematoxylin and eosin (H&E) staining and immunohistochemical (IHC) staining. The obtained pathological specimens were immersed in 10% neutral buffered formalin solution for fixation at room temperature (~22˚C) for 48 h, dehydrated through increasing ethanol series (75, 85, 95, 100 and 100%) and embedded in paraffin. After sectioning, deparaffinization and rehydration, the specimens were stained with 0.5% hematoxylin for 3-6 min and then with 0.5% eosin Y for 2-3 min, both at room temperature. Subsequently, the stained sections were dehydrated through a graded ethanol series, cleared in xylene and mounted with a neutral resin.

For IHC staining, the paraffin-embedded tumor sections were first deparaffinized in xylene (cat. no. 10023418; Sinopharm Chemical Reagent Co., Ltd.) and then rehydrated in a descending ethanol series (100, 100, 95, 85 and 75%) for 5 min each. Antigen retrieval was performed using heat-induced epitope retrieval at a pressure of 103 kPa and a temperature of 125˚C for 23 min. After a 10-min treatment with 3% hydrogen peroxide (cat. no. 10011218; Sinopharm Chemical Reagent Co., Ltd.) at room temperature, the cells were incubated in a humidified chamber for 30 min to eliminate endogenous peroxidase activity. The cells were then blocked with 10% goat serum (cat. no. SL038-10 ml; Beijing Solarbio Science & Technology Co., Ltd.) at room temperature for 30 min. The sections were incubated overnight at 4˚C with anti-SIVA-1 antibody (1:200; cat. no. PA5-100737; Thermo Fisher Scientific, Inc.). After washing with PBS, the slides were incubated with the ready-to-use HRP-Polymer Anti-Mouse/Rabbit reagent (cat. no. Kit-5020; MaxVision Biosciences) at 37˚C for 30 min according to the manufacturer's instructions. Detection was performed using a DAB substrate kit (cat. no. DA1010-2*3ml; Beijing Solarbio Science & Technology Co., Ltd.), after which the sections were counterstained with hematoxylin (cat. no. G1140; Beijing Solarbio Science & Technology Co., Ltd.). Subsequently, the sections were dehydrated in an increasing ethanol series (75, 85, 95, 100 and 100%) for 5 min each, and xylene was added for permeabilization (repeated twice, 3 min each time). The slides were then mounted using neutral resin and imaging was carried out using an optical microscope. The immunostaining scoring of each pathological section was performed by two independent pathologists, and IHC staining results were semi-quantified using the QuickScore scoring method (24). The IHC staining score consisted of the intensity of cell staining and the percentage of positively stained cells, where the intensity of cell staining was scored as follows: 0 (no staining), 1+ (weak staining), 2+ (moderate staining) and 3+ (strong staining). The percentage of positively stained cells was evaluated according to the following criteria: 0 (0%), 1 (<10%), 2 (10-25%), 3 (26-50%), 4 (51-75%) and 5 (>75%). The IHC staining score was calculated as the intensity of cell staining x the percentage of positively stained cells [score of 0-3 (-), score of 4-6 (+), score of 7-9 (++) and score of 10-12 (++++)].

Statistical analysis. R 4.2.3 (https://cran.r-project.org/bin/windows/base/old/4.2.3/) and SPSS 23.0 (IBM, Corp.) statistical software were used for analysis. Each experiment was independently repeated three times. The data from the IHC staining scores are presented as the median with the interquartile range, whereas continuous data are presented as the mean ± standard deviation. Differences between the groups were compared using one-way ANOVA, followed by Tukey's post hoc test to facilitate multiple comparisons. As the data from the IHC staining scores did not meet the key assumptions required for parametric tests (normal distribution and homogeneity of variance), the Kruskal-Wallis test was performed, followed by Dunn post hoc test for pairwise comparisons. $P<0.05$ was considered to indicate a statistically significant difference.

Results

Investigation of the expression profile of SIVA-1 and its relationship with drug sensitivity. First, differential gene analysis was performed using the GSE186205 dataset, and the results are shown in a volcano plot (Fig. 1A). SIVA-1 was differentially expressed in cisplatin-resistant gastric cancer cell lines, where its expression was lower compared with that in cisplatin-sensitive gastric cancer cell lines. The association between SIVA-1 and survival status was explored, and data visualization was performed by plotting risk factor associations using TCGA-STAD data. The results showed that when SIVA-1 expression was high, the risk score for a positive event (death) was high (risk score cut-off, >0.07). Specifically, the risk of death was 1.01 times higher in the high-expression group than in the low-expression group. (Fig. 1B). Therefore, high SIVA-1 expression could be considered a high-risk factor. KEGG enrichment analysis revealed that SIVA-1 was associated with the 'p53 signaling pathway' (Fig. 1C). In addition, GO enrichment analysis revealed that SIVA-1 was involved in the BP terms of 'tumor necrosis factor receptor binding' and 'CD27 receptor binding', among others, the MF terms of 'apoptotic signaling pathway' and 'extrinsic apoptotic signaling pathway', as well as other functions. The results of the drug sensitivity analysis using the GSE186205 dataset are shown in Fig. 1D-F. SIVA-1 expression was negatively correlated with the IC_{50} value of DDP ($R=-0.846$, $P<0.05$), whereas statistically significant correlations were not observed with ADM or VCR ($P>0.05$). This indicated that when SIVA-1 expression was lower, the resistant group was less sensitive to DDP.

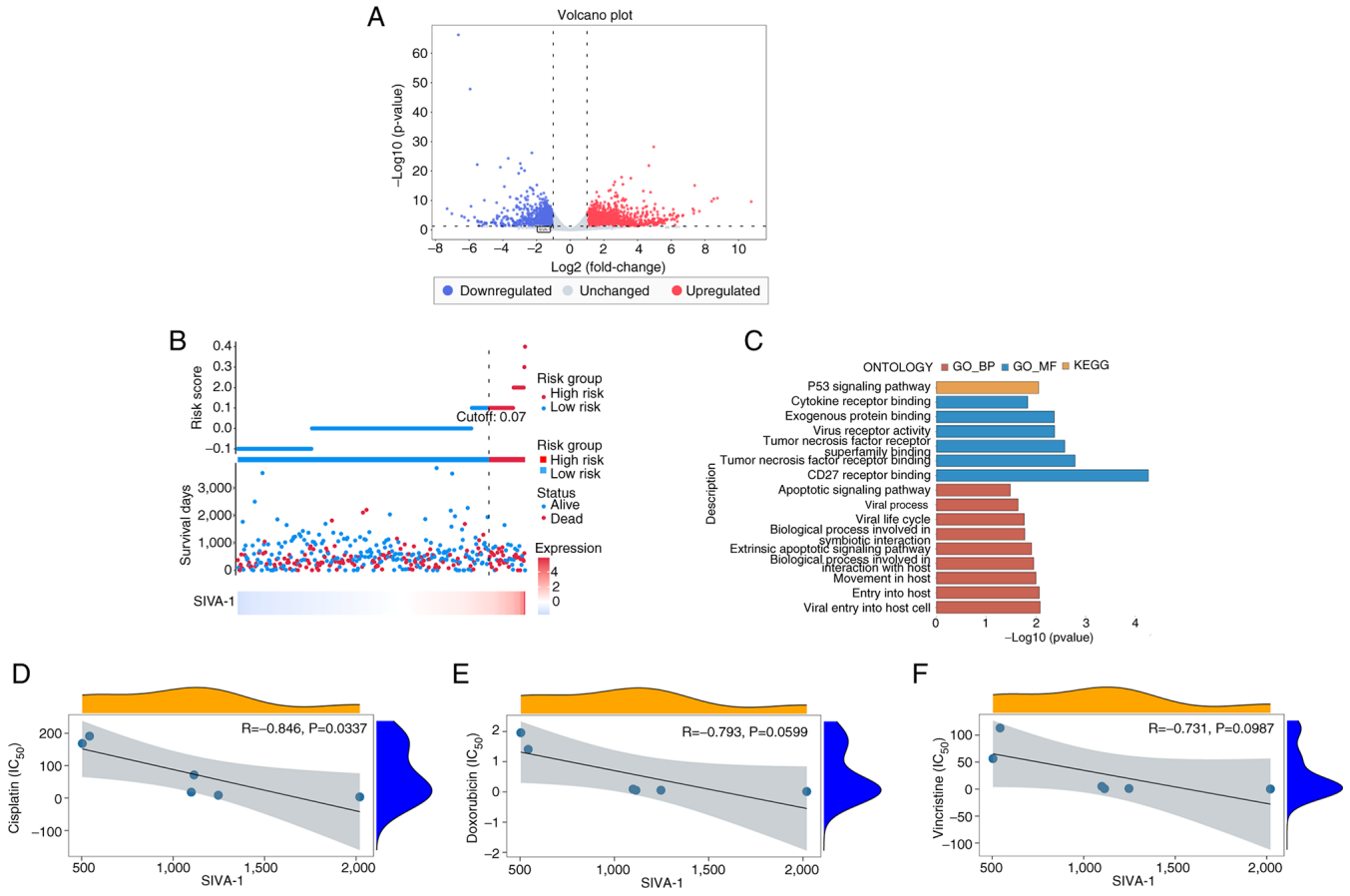

Figure 1. Bioinformatics analysis of SIVA-1. (A) Analysis of differentially expressed genes in the GSE186205 dataset. (B) Relationship between SIVA-1 and survival risk in TCGA-STAD dataset. (C) GO (BP, CC and MF) and KEGG enrichment analyses were performed on SIVA-1 in TCGA-STAD dataset. Drug sensitivity analyses of (D) cisplatin, (E) Adriamycin (doxorubicin) and (F) vincristine in the GSE186205 dataset. BP, biological process; CC, cellular component; GO, Gene Ontology; KEGG, Kyoto Encyclopedia of Genes and Genomes; MF, molecular function; TCGA-STAD, The Cancer Genome Atlas-stomach adenocarcinoma.

Obtaining and measuring the titers of shRNA-SIVA-1 and shRNA-NC lentiviral particles. The titer of shRNA-SIVA-1 and shRNA-NC lentiviral particles was measured by gradient dilution method to be $2x10^9$ TU/ml. Fluorescence-labeled lentiviruses were also observed by fluorescence microscopy and the viral titer was calculated using the following formula: Viral titer=number of fluorescent cells/volume of viral stock solution (Fig. 2A).

Infection of drug-resistant gastric cancer cells with shRNAs and screening of cell lines with stable SIVA-1 knockdown. The shRNA-SIVA-1 and shRNA-NC lentiviral particles contain the GFP reporter gene. They were infected into AGS/DDP cells to establish the shRNA-SIVA-1, shRNA-NC and control groups. The stable SIVA-1 knockdown cell line was then established from the GFP-positive cells from the shRNA-SIVA-1 group (Fig. 2B).

Expression of SIVA-1 in AGS/DDP cells. To assess the effects of the shRNA-SIVA-1 lentivirus on SIVA-1 expression following infection into AGS/DDP cells, the relative mRNA expression levels of SIVA-1 in each group of cells were measured by reverse transcription-quantitative PCR. The results showed that the mRNA levels of SIVA-1 were significantly decreased in the shRNA-SIVA-1 group compared with those in the shRNA-NC and control groups (P<0.05; Fig. 2C). These findings indicated that the shRNA-SIVA-1 lentivirus downregulated the mRNA expression levels of SIVA-1 in AGS/DDP cells. In addition, the protein expression levels of SIVA-1 were determined by western blotting. The protein levels of SIVA-1 were also significantly decreased in the shRNA-SIVA-1 group compared with in the shRNA-NC and control groups (P<0.05; Fig. 2D and E).

Silencing of SIVA-1 results in increased resistance to DDP in AGS/DDP cells. To investigate the effect of silencing SIVA-1 on drug resistance in resistant gastric cancer cells, the IC_{50} values of ADM, DDP and VCR in each group of cells was measured by performing at least three independent cell viability assays. The results showed that the IC_{50} value (μg/ml) of DDP in the shRNA-SIVA-1 group (21.43±0.52) was significantly increased compared with that in the control (17.49±0.30) and shRNA-NC (17.33±0.39) groups (P<0.05) (Table II). By contrast, the differences in the IC_{50} values of ADM and VCR were not significant between the cells in each group (P>0.05). These findings indicated that SIVA-1 knockdown could enhance the resistance AGS/DDP gastric cancer cells to DDP.

Silencing of SIVA-1 promotes the proliferation of AGS/DDP cells. To investigate the role of SIVA-1 in the proliferation

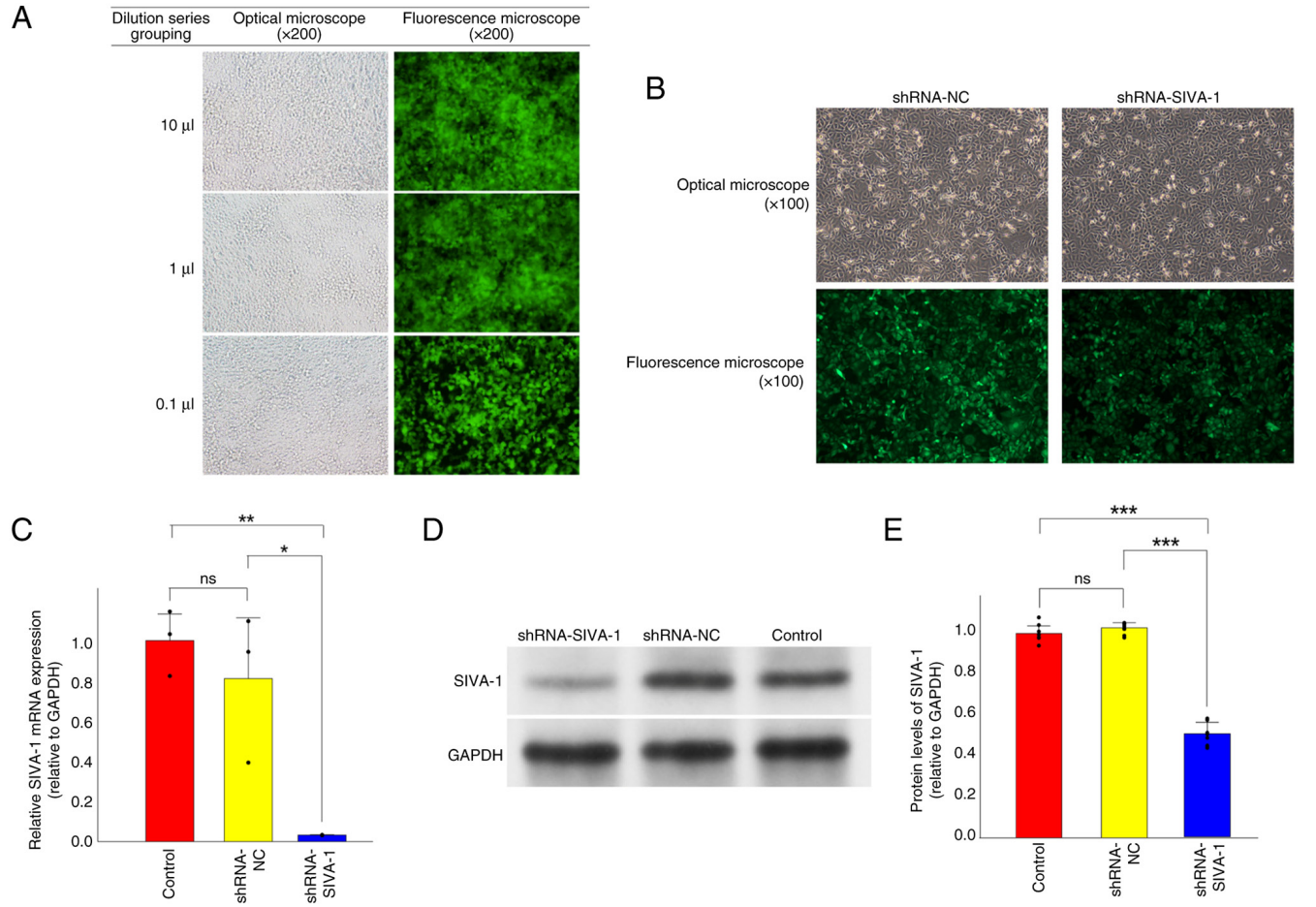

Figure 2. Generation and validation of stable SIVA-1-silenced AGS/DDP cells. (A) Infection efficiency of lentiviral plasmids at gradient dilution concentrations of 10, 1 and 0.1 μl is represented by GFP fluorescence intensity (original magnification, x200). (B) Effects of lentiviral infection on AGS/DDP cells (original magnification, x100). (C) mRNA expression levels of SIVA-1 in cells from each group, with GAPDH used as an internal reference. (D) Western blot analysis was performed to measure the protein expression levels of SIVA-1 in each group of cells. (E) Semi-quantification of SIVA-1 protein expression levels in cells from each group, with GAPDH used as an internal reference. The results indicate the ratio of the optical density of SIVA-1 bands to the optical density of GAPDH bands. *P<0.05, **P<0.01, ***P<0.001, as determined by ANOVA tests. DDP, cisplatin; NC, negative control; ns, not significant; shRNA, short hairpin RNA.

of AGS/DDP gastric cancer cells, a colony formation assay was performed (Fig. 3A and B). Compared with in the control (16.96±6.87%) and shRNA-NC (21.09±8.47%) groups, the colony formation rate was significantly higher in the shRNA-SIVA-1 group (51.84±4.51%) (P<0.05). These results indicated that SIVA-1 silencing could promote the proliferative function of DDP-resistant gastric cancer cells.

Silencing SIVA-1 induces apoptosis in AGS/DDP cells. The effects of silencing SIVA-1 on apoptosis in AGS/DDP cells were explored through at least three independent replicate experiments (Fig. 3C and D). The results demonstrated that the apoptosis rate in the shRNA-SIVA-1 group (23.84±0.94%) was significantly lower than that in the shRNA-NC (43.21±2.60%) and control (43.15±2.65%) groups (P<0.05). By contrast, no significant differences were observed between the shRNA-NC and control groups.

Silencing of SIVA-1 enhances the migration and invasion of AGS/DDP cells. Firstly, the effect of SIVA-1 silencing on the migration of AGS/DDP cells was assessed by scratch assay (Fig. 3E and F). According to the healing rate results at 48 h, the scratch healing rate of the shRNA-SIVA-1 group (74.54±5.08%) was significantly increased compared with that in the control (55.61±10.70%) and shRNA-NC (43.94±11.69%) groups (P<0.05). These findings suggested that silencing SIVA-1 could improve the mobility of DDP-resistant gastric cancer cells. In addition, using the Transwell assay, the effect of SIVA-1 silencing on the migration and invasion of AGS/DDP cells was investigated. As shown in Fig. 3G and H, the number of migrating cells was significantly increased in the shRNA-SIVA-1 group (931.78±38.28) relative to the shRNA-NC (612.56±53.92) and control (594.22±30.98) groups (P<0.05). The results of the invasion assay, shown in Fig. 3G and I, showed that the number of invasive cells in the shRNA-SIVA-1 group (928.78±57.93) was significantly higher compared with that in the shRNA-NC (467.00±74.15) and control (495.56±71.28) groups (P<0.05).

SIVA-1 silencing increases tumor burden in vivo. To further validate the biological role of SIVA-1 silencing in the gastric cancer environment *in vivo*, subcutaneous tumor loading experiments were performed in nude mice. The changes in the weight of the individual nude mice and the volume of the

Table II. Effect of SIVA-1 silencing on DDP, ADM and VCR resistance in AGS/DDP cells.

	IC_{50} values		
Drug	shRNA-SIVA-1	shRNA-NC	Control
DDP, μg/ml	21.43±0.52[a]	17.33±0.39[a]	17.49±0.30[a]
VCR, μg/ml	318.89±9.12	315.52±6.49	321.67±9.10
ADM, μg/ml	4.49±1.12	4.68±0.75	3.27±0.63

[a]P<0.05 vs. the shRNA-NC and control groups, analyzed by one-way ANOVA. ADM, Adriamycin; DDP, cisplatin; NC, negative control; shRNA, short hairpin RNA; VCR, vincristine.

subcutaneous tumors in each group were observed. In the final analysis, only three nude mice survived in each group, with some mice reaching pre-defined humane endpoints (due to severe injuries from fighting or complications of DDP chemotherapy) and were therefore euthanized. Throughout the entire experimental period, a total of four nude mice died as a result of in-fighting; among these, one was from the shRNA-SIVA-1 group, one from the shRNA-NC group and two from the control group. The results showed that the weight of tumors in the shRNA-SIVA-1 group (0.95±0.11 g) was significantly increased compared with that in the shRNA-NC (0.54±0.06 g) and control (0.39±0.19 g) groups (P<0.05; Fig. 4A and B). The growth rate of subcutaneous xenograft tumors in the shRNA-SIVA-1 group was significantly faster than that in the shRNA-NC and control groups (P<0.05; Fig. 4C). Fig. 4D shows the RTV on day 13. The RTV value of the shRNA-SIVA-1 group (4.55±0.73) was significantly higher than that in the shRNA-NC (2.92±0.12) and control (2.61±0.55) groups (P<0.05). Cell staining results are shown in Fig. 4E. Observing the paraffin-embedded sections of subcutaneous xenograft tumors in nude mice after H&E staining, the shRNA-SIVA-1 group showed abnormal cellular morphology with uneven nuclei sizes, and nuclear pleomorphism was observed in some areas. In addition, the results of the IHC staining showed that the expression of SIVA-1 in the subcutaneous metastases of nude mice in the shRNA-SIVA-1 group was lower than that in the shRNA-NC and control groups (P<0.05; Fig. 4F), indicating that SIVA-1 was silenced in the subcutaneous metastases of the shRNA-SIVA-1 group.

Screening of Bcl-2, BAX, XIAP, MAPK8 and BIRC5 as interaction genes of SIVA-1. To explore the genes associated with SIVA-1, GSEA was performed on the GSE186205 dataset. The two signaling pathways 'MicroRNAs in cancer' and 'Chemical carcinogenesis-receptor activation' were differentially expressed in cisplatin-resistant gastric cancer cell lines compared with those in cisplatin-sensitive gastric cancer cell lines in KEGG enrichment analyses (Fig. 5A). In GO enrichment analyses, 'mitochondrial protein-containing complex', 'protein localization to mitochondrion', 'apoptotic mitochondrial changes', 'regulation of release of cytochrome c from mitochondria', 'metaphase/anaphase transition of cell cycle' and 'regulation of endopeptidase activity' were differentially expressed in drug-resistant tissues (Fig. 5B). BAX was enriched in the following terms: 'mitochondrial protein-containing complex', 'protein localization to mitochondrion', 'apoptotic mitochondrial changes' and 'regulation of release of cytochrome c from mitochondria'. In addition, BIRC5 has the biological function of 'metaphase/anaphase transition of cell cycle' and 'regulation of endopeptidase activity'. In a previous study, experimental results showed that SIVA-1 affects the expression of Bcl-2 (25). Furthermore, the data in the previous study suggested that SIVA-1 influences apoptosis by interacting with XIAP and concomitantly regulating MAPK8 (26). Therefore, based on the GSEA, a GO enrichment analysis of Bcl-2, BAX, XIAP, MAPK8 and BIRC5 was performed to investigate the functions of these five genes. The results are shown in Fig. 5C; the GO enrichment analysis revealed that Bcl-2, BAX, XIAP, MAPK8 and BIRC5 were primarily enriched in the BP terms 'regulation of mitochondrial outer membrane permeabilization involved in apoptotic signaling pathway', 'regulation of intrinsic apoptotic signaling pathway in response to DNA damage by p53 class mediator', 'regulation of protein insertion into mitochondrial membrane involved in apoptotic signaling pathway' and 'intrinsic apoptotic signaling pathway in response to DNA damage'. The CC term 'Bcl-2 family protein complex' and 'mitochondrial outer membrane' indicated that Bcl-2 may form a protein complex with BAX and is located on the outer membrane of the mitochondria. The MF terms, particularly those related to protein binding ('BH3 domain binding' and 'death domain binding'), receptor binding ('CD27 receptor binding' and 'tumor necrosis factor receptor binding') and enzyme regulator activity ('cysteine-type endopeptidase inhibitor activity involved in apoptotic processes'), showed that the aforementioned five genes had the ability to regulate enzyme activities or bind to receptors. The gene expression correlation heatmap showed that SIVA-1 was correlated with MAPK8 (r=0.1, P<0.05), MAPK8 was correlated with Bcl-2 (r=0.2, P<0.05), Bcl-2 was correlated with XIAP (r=0.2, P<0.05) and with BIRC5 (r=-0.2, P<0.05), and BAX was correlated with XIAP (r=0.1, P<0.05) and BIRC5 (r=0.3, P<0.05), although these correlations were very weak (Fig. 5D). PPI networks (Fig. 5E), along with its visual legend (Fig. 5F), showed that SIVA1 acts as an upstream gene linked to MAPK8 by regulating MDM2, which indirectly regulates Bcl-2 and BAX, and ultimately affects XIAP and BIRC5.

Silencing of SIVA-1 upregulates the expression of Bcl-2, BIRC5, XIAP and MAPK8, and downregulates the expression of BAX. Combined with the protein interaction results

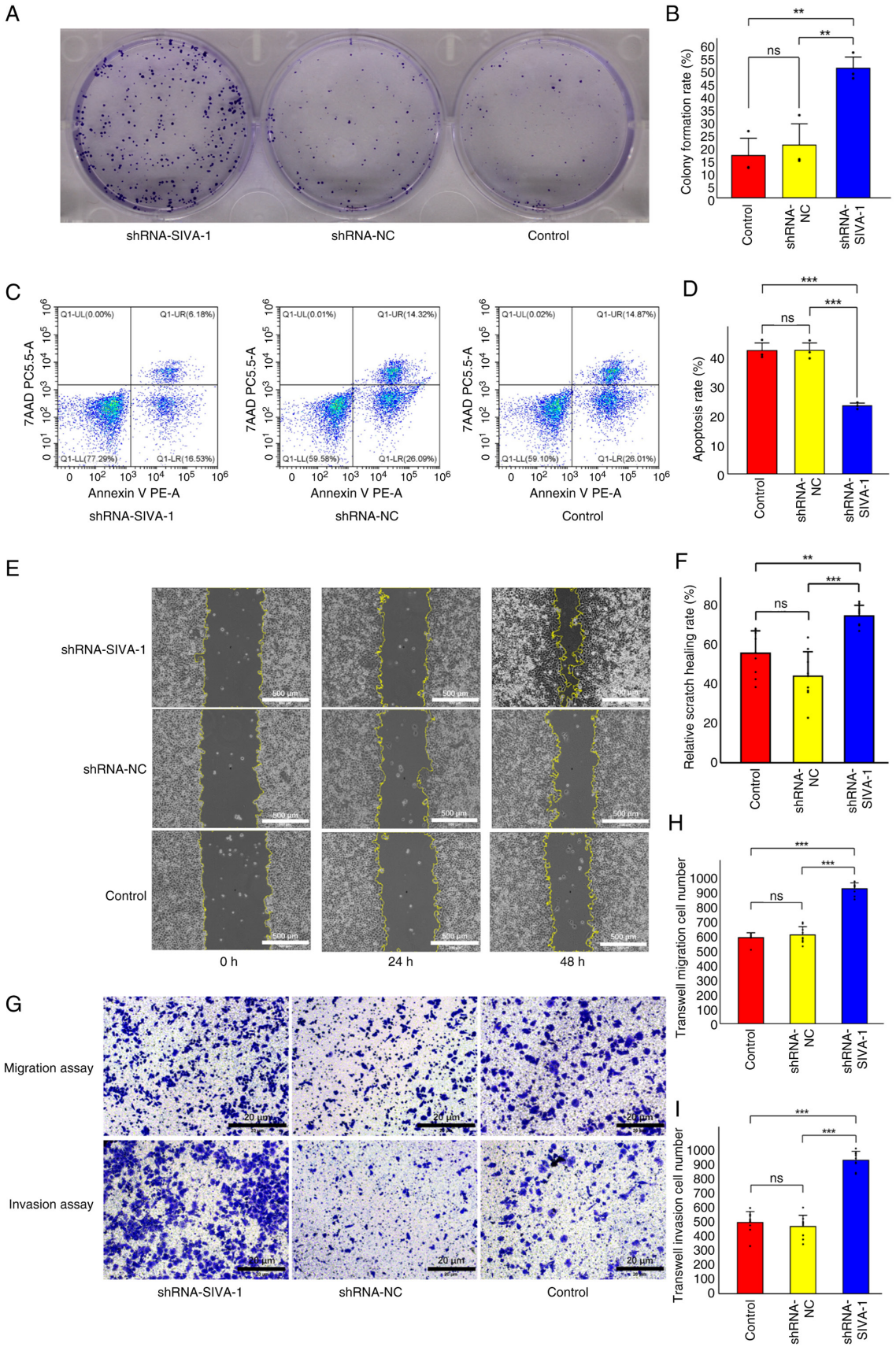

Figure 3. Effects of SIVA-1 silencing on various cellular functions of AGS/DDP cells. (A) Effect of SIVA-1 silencing on the proliferation of AGS/DDP gastric cancer cells was assessed by colony formation assay. (B) Colony formation rate of each group of cells after SIVA-1 silencing. (C) Effect of SIVA-1 silencing on the apoptosis of AGS/DDP gastric cancer cells was elucidated using an apoptosis assay. (D) Apoptosis rate of cells in each group following silencing of SIVA-1. (E) Effect of SIVA-1 silencing on the migration of AGS/DDP gastric cancer cells was demonstrated by cell scratch assay. (F) Healing rate of AGS/DDP cells at 48 h in each group after SIVA-1 silencing. (G) Effect of SIVA-1 silencing on the migration and invasion of AGS/DDP gastric cancer cells was assessed through Transwell assays. Numbers of (H) migratory and (I) invasive cells in each group after SIVA-1 silencing. **P<0.01, ***P<0.001, as determined by ANOVA tests. DDP, cisplatin; NC, negative control; ns, not significant; shRNA, short hairpin RNA.

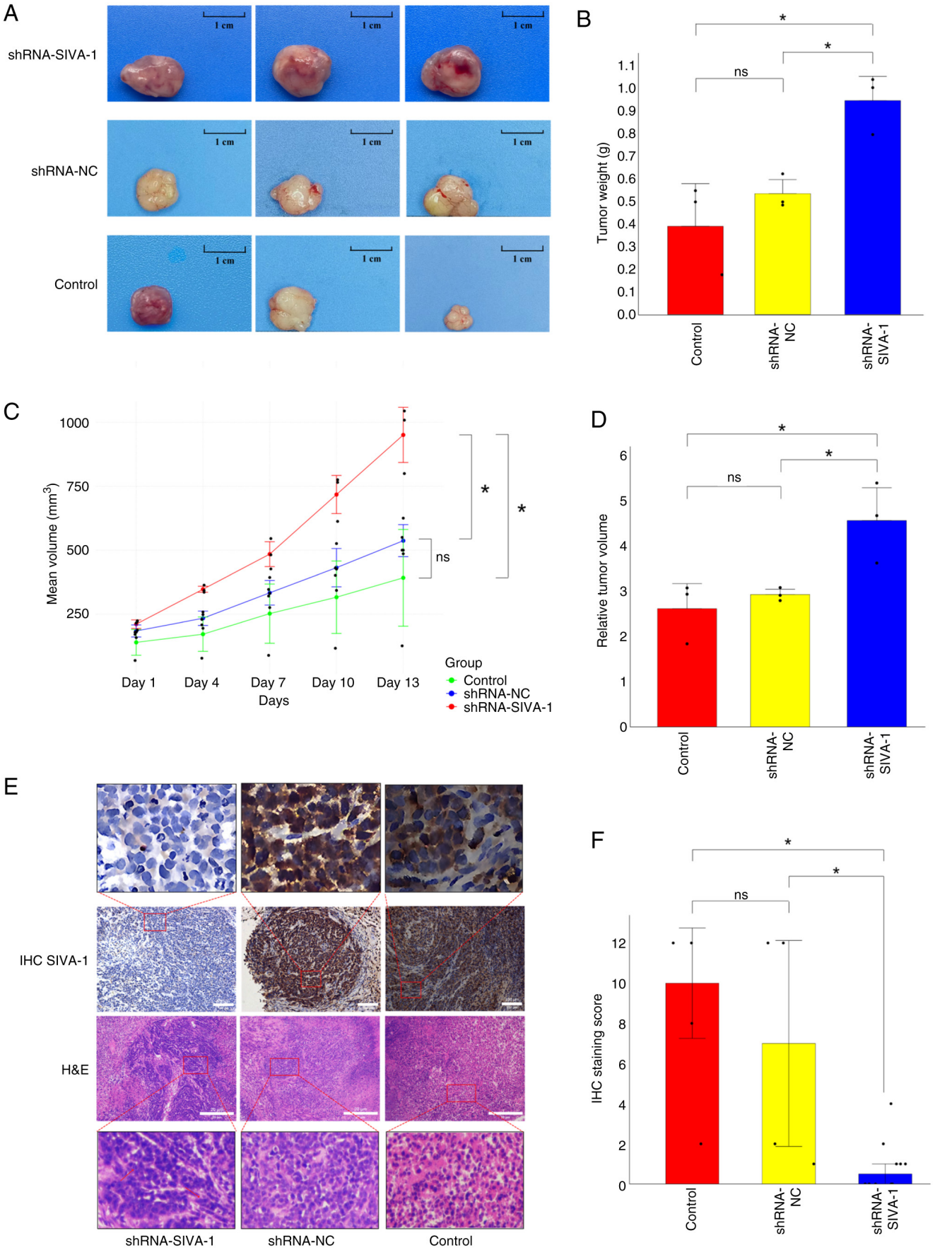

Figure 4. Silencing of SIVA-1 results in increased tumor burden. (A) Subcutaneous xenograft tumors removed from nude mice in each group 13 days after tumor injection. (B) Measurement of tumor weight of nude mice in each group 13 days after tumor injection. (C) Changes in subcutaneous transplanted tumor volume in nude mice. (D) Relative tumor volume on day 13 was measured in each group of nude mice. (E) H&E staining and IHC staining images of subcutaneous tumor tissues of nude mice in each group. (F) IHC staining scores for each group. *P<0.05, as determined by (B and D) ANOVA or (F) Kruskal-Wallis tests. H&E, hematoxylin and eosin; IHC, immunohistochemical; NC, negative control; ns, not significant; shRNA, short hairpin RNA.

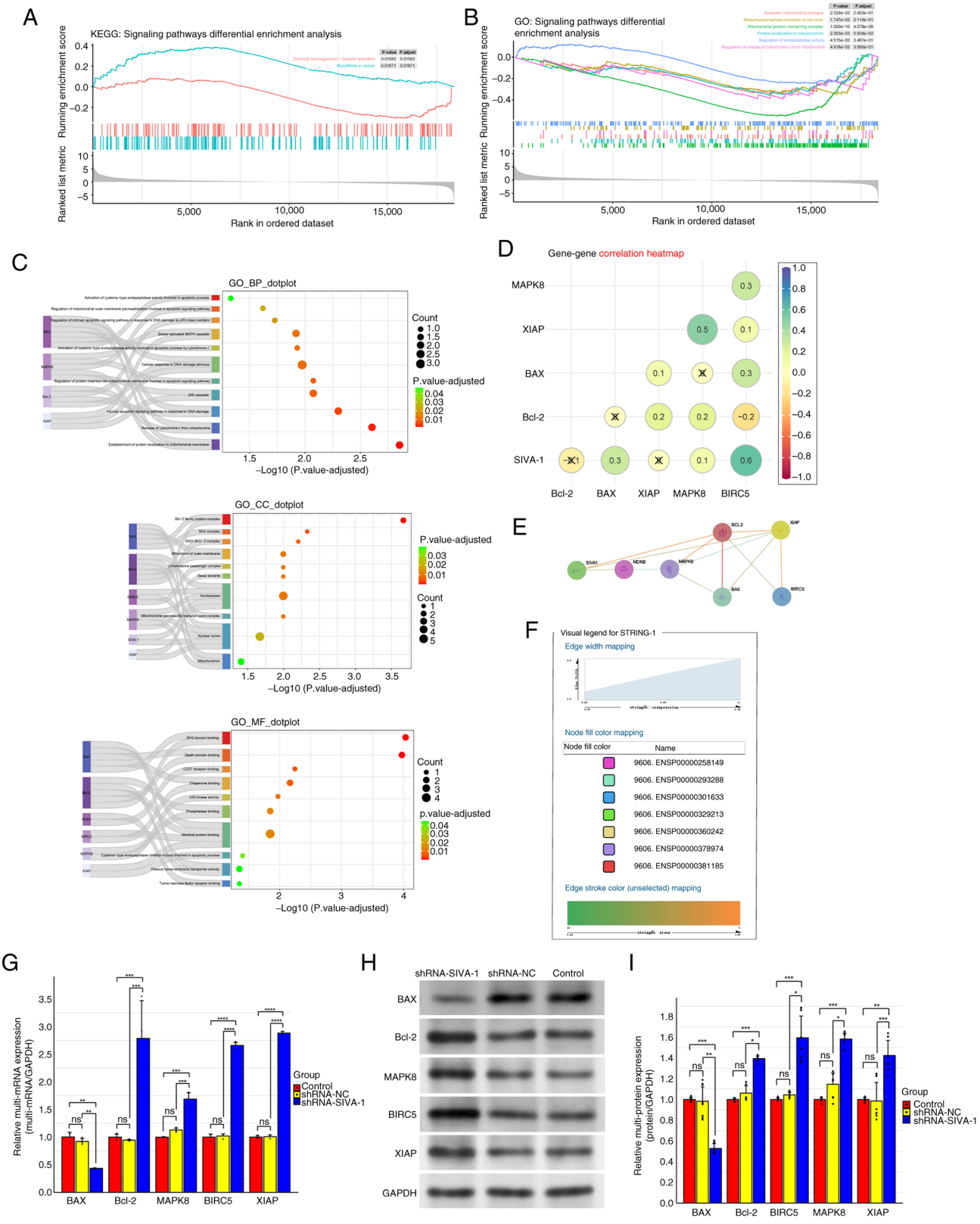

Figure 5. Analysis and validation of SIVA-1 interaction with Bcl-2, BAX, XIAP, MAPK8 and BIRC5, and related signaling pathways. (A) GSEA of KEGG pathways in the GSE186205 dataset. (B) GSEA of GO terms in the GSE186205 dataset. (C) BP, CC and MF terms associated with SIVA-1, Bcl-2, BAX, XIAP, MAPK8 and BIRC5, as determined by GO enrichment analysis in the GSE186205 dataset. (D) Gene expression correlation heatmap of SIVA-1, Bcl-2, BAX, XIAP, MAPK8 and BIRC5 in The Cancer Genome Atlas-stomach adenocarcinoma dataset. 'X' indicates P≥0.05. (E) Interactions between SIVA-1, and Bcl-2, BAX, XIAP, MAPK8 and BIRC5 proteins in the STRING 12.0 database. (F) Visual legend of the protein-protein interaction network. (G) mRNA expression levels of Bcl-2, BAX, XIAP, MAPK8 and BIRC5 in each group of cells, as detected by reverse transcription-quantitative PCR after SIVA-1 silencing. (H) Protein expression levels of Bcl-2, BAX, XIAP, MAPK8 and BIRC5, as detected by western blotting after SIVA-1 silencing in each group of cells. (I) Semi-quantification of the protein expression levels of Bcl-2, BAX, XIAP, MAPK8 and BIRC5 in different groups of cells (using GAPDH as an internal reference). *P<0.05, **P<0.01, ***P<0.001, ****P<0.0001, as determined by ANOVA tests. BP, biological process; CC, cellular component; BIRC5, baculoviral inhibitor of apoptosis repeat-containing 5; GO, Gene Ontology; GSEA, Gene Set-Enrichment Analysis; KEGG, Kyoto Encyclopedia of Genes and Genomes; MF, molecular function; ns, not significant; XIAP, X-linked inhibitor of apoptosis protein.

of bioinformatics analysis, the mechanism by which SIVA-1 knockdown led to enhanced drug resistance in AGS/DDP cells was investigated by detecting the expression levels of apoptosis-related genes and genes of apoptosis-related signaling pathways (Bcl-2, BAX, XIAP, MAPK8 and BIRC5). The mRNA expression levels of these genes were detected by reverse transcription-quantitative PCR. The results showed that compared with those in the control and shRNA-NC groups, the mRNA expression levels of Bcl-2, BIRC5, XIAP and MAPK8 were increased, whereas the mRNA expression levels of BAX were decreased in the shRNA-SIVA-1 group ($P<0.05$; Fig. 5G). The expression levels of the aforementioned apoptosis-related proteins were detected by western blotting. The results were similar to those of the reverse transcription-quantitative PCR, with the expression levels of Bcl-2, BIRC5, XIAP and MAPK8 proteins increased, and BAX protein decreased in the shRNA-SIVA-1 group ($P<0.05$; Fig. 5H and I). Fig. 6 demonstrates that silencing SIVA-1 indirectly increases the expression of MAPK8 through MDM2, thereby triggering the mitochondrial-dependent apoptosis pathway, which is mediated by the Bcl-2/BAX signaling pathway. It is specifically manifested as the upregulation of Bcl-2 and the downregulation of BAX, and XIAP and BIRC5 are downstream regulatory genes of BAX. Their simultaneous upregulation ultimately affects apoptosis mediated by the caspase family of proteins. Therefore, silencing SIVA-1 was shown to block the apoptotic pathway caused by DDP through the MAPK8/Bcl-2/BAX signaling pathway.

Discussion

SIVA-1 is a gene closely related to apoptosis. Under the environmental conditions of hyperbaric oxygen, apoptosis can be promoted in glioma cells by downregulating SIVA-1 expression (11). Existing evidence has suggested that SIVA-1 has the potential to influence drug resistance in various types of cancer, including gastric cancer, colorectal cancer (27), cervical cancer (28) and hepatocellular carcinoma (29).

Gastric cancer is one of the most common malignant tumors of the digestive system, and the leading treatment is radical surgical resection of the lesion. As the signs or clinical symptoms of patients with early gastric cancer are not obvious, according to Tan *et al* (30), ~70% of patients with gastric cancer are in the advanced stages of the disease at the time of diagnosis. For patients diagnosed with advanced gastric cancer, curative surgical treatment is no longer considered an appropriate option; instead, a comprehensive treatment plan centered on systemic chemotherapy is often initiated (31). In order to improve prognosis and survival, the use of combination chemotherapeutic drugs is preferred in the clinical treatment of patients with advanced gastric cancer (32). With the wide application of various chemical drugs in the treatment of gastric cancer, an increasing number of patients have experienced reduced effectiveness of therapeutic drugs (33), ultimately leading to the progression of advanced gastric cancer and a notable decrease in the survival of patients. To address chemotherapeutic drug resistance, the preliminary experimental results of the present study showed that SIVA-1 expression was positively associated with the inhibition rate of DDP in gastric cancer cells (34), leading to altered drug sensitivity by mechanisms which have not yet been elucidated. In the present study, SIVA-1 was used as an upstream target to study drug resistance; its effects on drug-resistant gastric cancer cells and the efficacy of chemotherapeutic drugs were investigated, and the mechanism of reversing the occurrence of drug resistance was explored.

Bioinformatics analysis showed that SIVA-1 was expressed at a low level in DDP-resistant gastric cancer cell lines and that the low level of expression predicted resistance to DDP. However, the Cox proportional hazards model revealed that higher SIVA-1 expression levels in patients with gastric cancer were associated with an increased risk of death. It may be hypothesized that SIVA-1 serves a dual role in both ordinary gastric cancer cells and cisplatin-resistant gastric cancer cells. As demonstrated in earlier studies, the upregulation of SIVA-1, mediated by the long non-coding RNA FTX/microRNA-215-3p regulatory axis, promotes gastric cancer cell proliferation (35). By contrast, a review by Parducci *et al* (36) indicated that SIVA-1 can promote apoptosis in gastric cancer and enhance the effectiveness of chemotherapy. Nevertheless, the results of the present study showed that silencing SIVA-1 in AGS/DDP cells promoted their proliferation, migration and invasion. In addition, an inextricable association with endogenous apoptosis was suggested. It was also observed that the resistance of AGS/DDP cells to DDP was enhanced after silencing SIVA-1, which further confirmed the effect of SIVA-1 on the drug resistance of gastric cancer cells.

Preliminary evidence has indicated that SIVA-1 affects gastric cancer DDP resistance by regulating MDM2 expression (34). A previous study demonstrated that MAPK8 is a downstream target gene of MDM2 (37). Analysis of the PPI network diagram in the current study showed that SIVA-1 had an indirect effect on MAPK8 and was associated with MDM2; this led to the conclusion that SIVA1 indirectly regulates MAPK8 via MDM2. MAPK8, also termed c-Jun N-terminal kinase, may be considered a tumor resistance gene with a positive effect on eliminating tumor cells, which can be activated by tumor necrosis factor and in turn triggers the process of apoptosis (38). In addition, MAPK8 has been reported to affect the biological functions of tumor cells through multiple pathways, including proliferation, migration and apoptosis (39). The bioinformatics analysis results indicated that MAPK8, as a co-interacting protein with SIVA-1, may be involved in the regulation of endogenous apoptotic processes, which ultimately leads to a decrease in drug sensitivity of drug-resistant gastric cancer cells.

According to a previous study, MAPK8 indirectly inhibits apoptosis in hepatocellular carcinoma through the phosphorylation of Bcl-2 (40), and the key factor that influences apoptosis is the Bcl-2/BAX ratio. It is well established that Bcl-2 is an anti-apoptotic gene and that Bax is a pro-apoptotic gene (41), both of which belong to the Bcl-2 family of proteins. The MF term 'mitochondrial outer membrane', as determined by GO enrichment analysis, indicated that both Bcl-2 and BAX are located on the outer mitochondrial membrane and belong to the same key hub of the mitochondria-dependent apoptosis pathway. It has been suggested that an altered Bcl-2/BAX ratio in gastric cancer affects the mitochondria-dependent apoptotic pathway mediated by caspase family proteins (42). Low *et al* (43) observed that tumor cells develop drug resistance

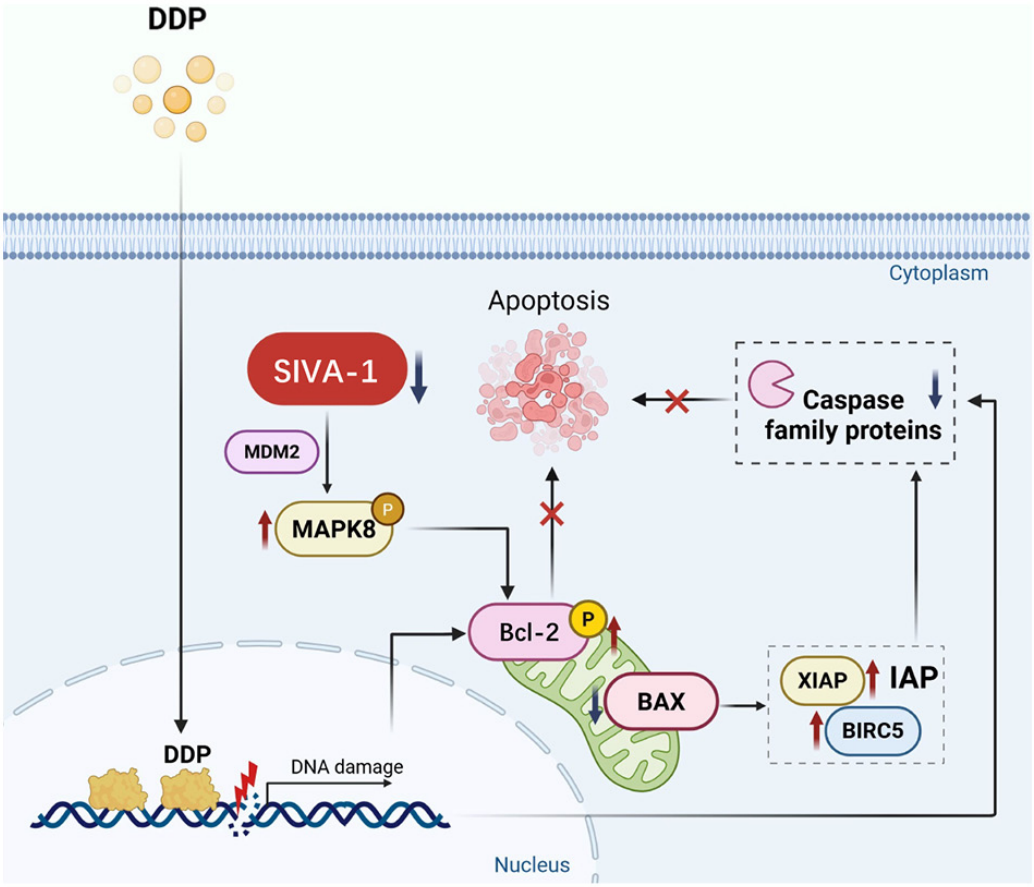

Figure 6. Schematic diagram illustrating the signaling pathway by which SIVA-1 silencing blocks DDP-induced apoptosis. BIRC5, baculoviral inhibitor of apoptosis repeat-containing 5; DDP, cisplatin; XIAP, X-linked inhibitor of apoptosis protein.

due to reduced apoptosis as a result of reduced accumulation of BAX in mitochondria, where the onset of apoptosis may be related to endogenous apoptosis mediated by caspase family proteins. Similarly, inhibition of Bcl-2 in acute myeloid leukemia results in increased drug sensitivity through activation of the mitochondrial autophagy process mediated by the BH3 structural domain (44). The results of the apoptosis assay in the present study demonstrated that silencing the expression of SIVA-1 in AGS/DDP cells hindered their progression through apoptosis. This ultimately resulted in an augmentation of the resistance of AGS/DDP cells to DDP. This result may be due to the activation of MAPK8/Bcl-2/BAX-mediated mitochondria-dependent apoptosis by SIVA-1.

XIAP, as a gene downstream of BAX (45), is responsible for regulating caspase family proteins and indirectly inhibiting the mitochondria-dependent apoptosis pathway. XIAP is considered to be an anti-apoptotic gene, similar to Bcl-2. One study showed that simultaneous inhibition of XIAP with Bcl-2 resulted in a higher rate of apoptosis in bladder cancer cells than inhibition of XIAP or Bcl-2 alone (46). Previous evidence has suggested that XIAP inhibits activation of the caspase family of proteins, which in turn regulates apoptosis. BIRC5 and XIAP belong to the IAP proteins family. Similar to XIAP, BIRC5 acts as a downstream gene of BAX (47), XIAP and BIRC5 work synergistically to affect cell function (48). The BIR structural domain is often considered to be a characteristic structure of the IAP family of proteins (49), and is associated with drug resistance (50). In addition, BIRC5 benefits from a unique BIR structural domain that directly inhibits mitochondria-dependent apoptosis by interacting with caspase family proteins (51). Similarly, Zhu *et al* (52) reported that overexpression of BIRC5 can increase drug resistance in lung cancer and suggested that this was caused by dysregulation of the apoptotic pathway.

In conclusion, the present study aimed to validate the effects of silencing SIVA-1 on the sensitivity of AGS/DDP cells to DDP, and to further investigate the mechanisms of enhancement of drug resistance and changes in tumor cell biological functions. A total of five genes associated with mitochondrial apoptotic pathways, MAPK8, Bcl-2, BAX, XIAP and BIRC5, were identified using bioinformatics analysis. In addition, using cellular experiments and constructing *in vivo* xenograft tumor model experiments, it was revealed that silencing SIVA-1 expression caused an increase in the expression levels of MAPK8, Bcl-2, XIAP and BIRC5 proteins, and a decrease in the expression level of BAX protein. Furthermore, an increase in resistance to DDP was observed. It was thus indicated that SIVA-1 acts indirectly on MAPK8, which in turn activates the Bcl-2/BAX-mediated mitochondria-dependent apoptosis pathway, with XIAP and BIRC5 acting as downstream target genes of BAX that synergize with caspase family proteins. Ultimately, it alters the biological function of gastric cancer-resistant cells and their sensitivity to chemotherapeutic agents. Thus, it is clear that SIVA-1 is a central gene affecting drug resistance in gastric cancer cells.

Acknowledgements

Not applicable.

Funding

The study was funded by the Natural Science Foundation of China (grant no. 82260468), the Natural Science Foundation of Guangxi (grant nos. 2023GXNSFAA026341, 2023GXNSFAA026143 and 2025GXNSFAA069965), the National Natural Science Foundation Cultivation Fund of the People's Hospital of Guangxi Zhuang Autonomous Region (grant nos. NSFC-HCF2025012 and 2026GPY0209) and the Guangxi Medical and Health Appropriate Technology Development and Promotion Project (grant no. S2024006).

Availability of data and materials

The data generated in the present study may be requested from the corresponding author.

Authors' contributions

XTW and FBK confirm the authenticity of all the raw data. ZYS, ZRD, LJX, SX, FBK and XTW contributed to the conception and design of the study. YQ, YLH, YRL, HBH, MRD, XGZ, XML, LL and XDD were involved in the acquisition, analysis and interpretation of the data. ZYS, LJX, ZRD, SX, LL, FBK and XTW drafted the manuscript. YQ, XW, FBK, XGZ and LL critically revised the manuscript for important intellectual content. All authors read and approved the final manuscript.

Ethics approval and consent to participate

The present study obtained approval from The Medical Ethics Committee of Guangxi Zhuang Autonomous Region People's Hospital (Nanning, China; approval no. KY-GZR-2016-416).

Patient consent for publication

Not applicable.

Competing interests

The authors declare that they have no competing interests.

References

1. Qin N, Fan Y, Yang T, Yang Z and Fan D: The burden of Gastric Cancer and possible risk factors from 1990 to 2021, and projections until 2035: Findings from the Global Burden of Disease Study 2021. Biomark Res 13: 5, 2025.
2. Siegel RL, Giaquinto AN and Jemal A: Cancer statistics, 2024. CA Cancer J Clin 74: 12-49, 2024.
3. Gupta J, Ahmed AT, Tayyib NA, Zabibah RS, Shomurodov Q, Kadheim MN, Alsaikhan F, Ramaiah P, Chinnasamy L and Samarghandian S: A state-of-art of underlying molecular mechanisms and pharmacological interventions/nanotherapeutics for cisplatin resistance in gastric cancer. Biomed Pharmacother 166: 115337, 2023.
4. Liu Q, Song Y, Su J, Yang S, Lian Q, Wang T, Wei H and Fang J: PUF60 promotes chemoresistance through drug efflux and reducing apoptosis in gastric cancer. Int J Med Sci 22: 269-282, 2025.
5. Ji N, Li H, Zhang Y, Li Y, Wang P, Chen X, Liu YN, Wang JQ, Yang Y, Chen ZS, *et al*: Lansoprazole (LPZ) reverses multidrug resistance (MDR) in cancer through impeding ATP-binding cassette (ABC) transporter-mediated chemotherapeutic drug efflux and lysosomal sequestration. Drug Resist Updat 76: 101100, 2024.
6. Chen H, Li Y, Li H, Chen X, Fu H, Mao D, Chen W, Lan L, Wang C, Hu K, *et al*: NBS1 lactylation is required for efficient DNA repair and chemotherapy resistance. Nature 631: 663-669, 2024.
7. Babaei S, Nikbakht M, Majd A and Mousavi SA: Comparative effects of arsenic trioxide and chemotherapy on Chk1 and CDC25 gene expression in gastric cancer cells AGS and MKN45: A potential therapeutic strategy. Mol Biol Rep 52: 198, 2025.
8. Xu F, Xu A, Guo Y, Bai Q, Wu X, Ji SP and Xia RX: PM2.5 exposure induces alveolar epithelial cell apoptosis and causes emphysema through p53/Siva-1. Eur Rev Med Pharmacol Sci 24: 3943-3950, 2020.
9. Li N, Jiang P, Du W, Wu Z, Li C, Qiao M, Yang X and Wu M: Siva1 suppresses epithelial-mesenchymal transition and metastasis of tumor cells by inhibiting stathmin and stabilizing microtubules. Proc Natl Acad Sci USA 108: 12851-1286, 2011.
10. Ma Y, Liu T, Song X, Tian Y, Wei Y, Wang J, Li X and Yang X: Siva 1 inhibits proliferation, migration and invasion by phosphorylating Stathmin in ovarian cancer cells. Oncol Lett 14: 1512-1518, 2017.
11. Ren ZQ, Wang RD, Wang C, Ren XH, Li DG, Liu YL and Yu QH: Key genes involved in the beneficial mechanism of hyperbaric oxygen for glioblastoma and predictive indicators of hyperbaric oxygen prolonging survival in glioblastoma patients. Curr Med Sci 44: 1036-1046, 2024.
12. Kong F, Wu K, Pang L, Huang Y, Li L, Xu J, Li F, Qing Y, Wang Z, Huang X, *et al*: Inhibition of apoptosis-regulatory protein Siva-1 reverses multidrug resistance in gastric cancer by targeting PCBP1. Oncol Res 30: 277-288, 2023.
13. Kong FB, Deng QM, Deng HQ, Dong CC, Li L, He CG, Wang XT, Xu S and Mai W: Siva-1 regulates multidrug resistance of gastric cancer by targeting MDR1 and MRP1 via the NF-κB pathway. Mol Med Rep 22: 1558-1566, 2020.
14. Phoo NLL, Dejkriengkraikul P, Khaw-On P and Yodkeeree S: Transcriptomic profiling reveals AKR1C1 and AKR1C3 mediate cisplatin resistance in signet ring cell gastric carcinoma via autophagic cell death. Int J Mol Sci 22: 12512, 2021.
15. Love MI, Huber W and Anders S: Moderated estimation of fold change and dispersion for RNA-seq data with DESeq2. Genome Biol 15: 550, 2014.
16. Maeser D, Gruener RF and Huang RS: oncoPredict: An R package for predicting in vivo or cancer patient drug response and biomarkers from cell line screening data. Brief Bioinform 22: bbab260, 2021.
17. Yu G, Wang LG, Han Y and He QY: clusterProfiler: An R package for comparing biological themes among gene clusters. OMICS 16: 284-287, 2012.
18. Livak KJ and Schmittgen TD: Analysis of relative gene expression data using real-time quantitative PCR and the 2(-Delta Delta C(T)) method. Methods 25: 402-408, 2001.
19. Weber EM, Zidar J, Ewaldsson B, Askevik K, Udén E, Svensk E and Törnqvist E: Aggression in Group-housed male mice: A systematic review. Animals (Basel) 13: 143, 2022.
20. Lidster K, Owen K, Browne WJ and Prescott MJ: Cage aggression in group-housed laboratory male mice: An international data crowdsourcing project. Sci Rep 9: 15211, 2019.
21. Van Loo PL, Van Zutphen LF and Baumans V: Male management: Coping with aggression problems in male laboratory mice. Lab Anim 37: 300-313, 2003.
22. CCAC Guidelines: Mice. A4, 118 pages. Canadian Council on Animal Care, 2019. Available at: https://ccac.ca/Documents/Standards/Guidelines/CCAC_Guidelines_Mice-Sept2022.pdf.
23. Workman P, Aboagye EO, Balkwill F, Balmain A, Bruder G, Chaplin DJ, Double JA, Everitt J, Farningham DA, Glennie MJ, *et al*: Guidelines for the welfare and use of animals in cancer research. Br J Cancer 102: 1555-1577, 2010.
24. Detre S, Saclani Jotti G and Dowsett M: A 'quickscore' method for immunohistochemical semiquantitation: Validation for oestrogen receptor in breast carcinomas. J Clin Pathol 48: 876-878, 1995.
25. Kong FB, Shi ZY, Huang YL, Chen HH, Deng QM, Wu K, Zhu Z, Li L, Xu S, Zhong XG, *et al*: SIVA-1 interaction with PCBP1 serves as a predictive biomarker for cisplatin sensitivity in gastric cancer and its inhibitory effect on tumor growth in vivo. J Cancer 15: 4301-4312, 2024.

26. Resch U, Schichl YM, Winsauer G, Gudi R, Prasad K and de Martin R: Siva1 is a XIAP-interacting protein that balances NFkappaB and JNK signalling to promote apoptosis. J Cell Sci 122: 2651-2661, 2009.
27. Lin Z, Wan AH, Sun L, Liang H, Niu Y, Deng Y, Yan S, Wang QP, Bu X, Zhang X, *et al*: N6-methyladenosine demethylase FTO enhances chemo-resistance in colorectal cancer through SIVA1-mediated apoptosis. Mol Ther 31: 517-534, 2023.
28. Liu T, Ma Y, Wang Z, Zhang W and Yang X: Siva 1 inhibits cervical cancer progression and its clinical prognosis significance. Cancer Manag Res 12: 303-311, 2020.
29. Li T, Lv M, Chen X, Yu Y, Zang G and Tang Z: Plumbagin inhibits proliferation and induces apoptosis of hepatocellular carcinoma by downregulating the expression of SIVA. Drug Des Devel Ther 13: 1289-1300, 2019.
30. Tan Z: Recent advances in the surgical treatment of advanced gastric cancer: A review. Med Sci Monit 25: 3537-3541, 2019.
31. Guan WL, He Y and Xu RH: Gastric cancer treatment: Recent progress and future perspectives. J Hematol Oncol 16: 57, 2023.
32. Takahari D: Second-line chemotherapy for patients with advanced gastric cancer. Gastric Cancer 20: 395-406, 2017.
33. Zhang W, Chen J, Wei Z, Song J, Zha X, Wang D and Xu M: Advancements and challenges in immunotherapy for gastric cancer: Current approaches and future directions. Front Immunol 16: 1592733, 2025.
34. Wang XT, Li L, Kong FB, Zhong XG and Mai W: Lentivirus-mediated overexpression of SIVA-1 reverses cisplatin resistance in gastric cancer in vitro. Cell Biochem Biophys 78: 455-463, 2020.
35. Zhang F, Wang XS, Tang B, Li PA, Wen Y and Yu PW: Long non-coding RNA FTX promotes gastric cancer progression by targeting miR-215. Eur Rev Med Pharmacol Sci 24: 3037-3048, 2020.
36. Parducci NS, Garnique ADMB, de Almeida BO and Machado-Neto JA: Exploring the dual role of SIVA1 in cancer biology. Gene 950: 149365, 2025.
37. Gao X, Wei M, Shan W, Liu Q, Gao J, Liu Y, Zhu S and Yao H: An oral 2-hydroxypropyl-β-cyclodextrin-loaded spirooxindole-pyrrolizidine derivative restores p53 activity via targeting MDM2 and JNK1/2 in hepatocellular carcinoma. Pharmacol Res 148: 104400, 2019.
38. Heaton WL, Senina AV, Pomicter AD, Salama ME, Clair PM, Yan D, Bell RN, Gililland JM, Prchal JT, O'Hare T and Deininger MW: Autocrine Tnf signaling favors malignant cells in myelofibrosis in a Tnfr2-dependent fashion. Leukemia 32: 2399-2411, 2018.
39. Parra E, Gutiérrez L and Ferreira J: Inhibition of basal JNK activity by small interfering RNAs enhances cisplatin sensitivity and decreases DNA repair in T98G glioblastoma cells. Oncol Rep 33: 413-418, 2015.
40. Chen S, Du Y, Xu B, Li Q, Yang L, Jiang Z, Zeng Z and Chen L: Vaccinia-related kinase 2 blunts sorafenib's efficacy against hepatocellular carcinoma by disturbing the apoptosis-autophagy balance. Oncogene 40: 3378-3393, 2021.
41. Adams JM and Cory S: Life-or-death decisions by the Bcl-2 protein family. Trends Biochem Sci 26: 61-66, 2001.
42. Chen J, Ji Z, Wu D, Wei S, Zhu W, Peng G, Hu M, Zhao Y and Wu H: MYBL2 promotes cell proliferation and inhibits cell apoptosis via PI3K/AKT and BCL2/BAX/Cleaved-caspase-3 signaling pathway in gastric cancer cells. Sci Rep 15: 9148, 2025.
43. Low HB, Wong ZL, Wu B, Kong LR, Png CW, Cho YL, Li CW, Xiao F, Xin X, Yang H, *et al*: DUSP16 promotes cancer chemoresistance through regulation of mitochondria-mediated cell death. Nat Commun 12: 2284, 2021.
44. Glytsou C, Chen X, Zacharioudakis E, Al-Santli W, Zhou H, Nadorp B, Lee S, Lasry A, Sun Z, Papaioannou D, *et al*: Mitophagy promotes resistance to BH3 mimetics in acute myeloid leukemia. Cancer Discov 13: 1656-1677, 2023.
45. An HG, Shin S, Lee B, Kwon Y, Kwon TU, Kwon YJ and Chun YJ: Induction of synergistic apoptosis by tetramethoxystilbene and nutlin-3a in human cervical cancer cells. Toxicol Res 38: 591-600, 2022.
46. Kunze D, Kraemer K, Erdmann K, Froehner M, Wirth MP and Fuessel S: Simultaneous siRNA-mediated knockdown of anti-apoptotic BCL2, Bcl-xL, XIAP and survivin in bladder cancer cells. Int J Oncol 41: 1271-1277, 2012.
47. Al-Astani Tengku Din TA, Shamsuddin SH, Idris FM, Ariffin Wan Mansor WN, Abdul Jalal MI and Jaafar H: Rapamycin and PF4 induce apoptosis by upregulating Bax and down-regulating survivin in MNU-induced breast cancer. Asian Pac J Cancer Prev 15: 3939-3944, 2014.
48. Hehlgans S, Petraki C, Reichert S, Cordes N, Rödel C and Rödel F: Double targeting of Survivin and XIAP radiosensitizes 3D grown human colorectal tumor cells and decreases migration. Radiother Oncol 108: 32-39, 2013.
49. Berthelet J and Dubrez L: Regulation of apoptosis by inhibitors of apoptosis (IAPs). Cells 2: 163-187, 2013.
50. Shi L, Lu J, Xia X, Liu X, Li H, Li X, Zhu J, Li X, Sun H and Yang X: Clinically used drug arsenic trioxide targets XIAP and overcomes apoptosis resistance in an organoid-based preclinical cancer model. Chem Sci 15: 8311-8322, 2024.
51. Pavlyukov MS, Antipova NV, Balashova MV, Vinogradova TV, Kopantzev EP and Shakhparonov MI: Survivin monomer plays an essential role in apoptosis regulation. J Biol Chem 286: 23296-23307, 2011.
52. Zhu X, Zhou R, Lu Y, Zhang Y, Chen Q and Li Y: Identification and validation of afatinib potential drug resistance gene BIRC5 in Non-Small cell lung cancer. Front Oncol 11: 763035, 2021.